Multiobjective Distributed Array Beamforming in the Near Field Using Wireless Syntonization

Ahona Bhattacharyya, Graduate Student Member, IEEE, Jason M. Merlo[®], Graduate Student Member, IEEE, Serge R. Mghabghab[®], Member, IEEE, Anton Schlegel[®], Graduate Student Member, IEEE, and Jeffrey A. Nanzer[®], Senior Member, IEEE

Abstract—We demonstrate the efficacy of distributed microwave multiobjective beamforming at ranges near field to the array using an optimization algorithm and wireless frequency alignment (syntonization). While considerable research has recently been devoted to distributed phased array coordination, the ability to steer signals to locations close to the array in open-loop (feedback-free) systems has not been demonstrated. In this work, we apply a traditional far-field beamforming algorithm to a set of distributed antennas that are wirelessly syntonized. We demonstrate multiobjective beamforming at 0.9 GHz using software-defined radios (SDRs) in a distributed array steering either two beams (focii) or one beam and one null. This work demonstrates the feasibility of a critical part of future distributed beamforming systems that, when combined with other coordination technologies, will support coherent beamforming in widely distributed wireless systems.

Index Terms—Distributed beamforming, distributed phased arrays, multiobjective beamforming, near-field beamforming, wireless frequency syntonization.

I. INTRODUCTION

CORDINATING the wireless functionality of separate electromagnetic systems enables a range of capability improvements compared with single-platform wireless systems [1], [2], [3]. When coordinated at the level of the radio frequency (RF) wavelength, coherent distributed beamforming operations are possible [4], in which transmit gain scales proportionally to the square of the number of transmitters due to the aggregate signal power and beamforming gain and scales proportionally to the number of receivers due to beamforming gain on receive. An array of N transmitters and M receivers can obtain an increased gain of up to N^2M compared with a single node, yielding dramatic increases in signal-to-noise

Manuscript received 6 October 2022; revised 7 November 2022; accepted 19 November 2022. Date of publication 3 February 2023; date of current version 7 June 2023. This work was supported in part by the Defense Advanced Research Projects Agency under Grant HR00112010015, in part by the Office of Naval Research under Grant N00014-20-1-2389, and in part by the National Science Foundation under Grant 1751655. (Corresponding author: Jeffrey A. Nanzer.)

Ahona Bhattacharyya, Jason M. Merlo, Anton Schlegel, and Jeffrey A. Nanzer are with the Department of Electrical and Computer Engineering, Michigan State University, East Lansing, MI 48824 USA (e-mail: bhatta67@msu.edu; merlojas@msu.edu; schleg19@msu.edu; nanzer@msu.edu).

Serge R. Mghabghab was with the Department of Electrical and Computer Engineering, Michigan State University, East Lansing, MI 48824 USA. He is now with MathWorks, Natick, MA 01760 USA (e-mail: mghabgha@msu.edu). Color versions of one or more figures in this letter are available at https://doi.org/10.1109/LMWT.2022.3231183.

Digital Object Identifier 10.1109/LMWT.2022.3231183

ratio, and thereby improving communications throughput, sensing performance, and other wireless capabilities.

Coordination in distributed antenna arrays requires accurate alignment of the electrical states of the elements in the array. Feedback-based coordination approaches use a destination node to provide information on the beamformed signal quality to the array in a closed-loop fashion [5], [6]; however, these approaches can only reliably direct signals to the location of the feedback, and thus remote sensing, radar, passive sensing, and other applications are not feasible. In this work, we focus on technologies supporting feedback-free, or openloop, distributed beamforming, where the array aligns itself without external inputs [7]. Open-loop systems are more challenging to coordinate but allow beamforming to arbitrary directions and support any wireless application. Distributed array coordination requires the nodes to be: phase coherent, ensuring that beamformed signals arrive at the destination in-phase, which necessitates accurate relative position estimation [8]; frequency syntonized, ensuring that the signals stay phase-coherent over the course of the waveform [9]; and time synchronized, ensuring that the signal information is sufficiently aligned [10]. In widely distributed systems, beamforming may also occur in the near field of the array.

In this letter, we demonstrate the feasibility of multiobjective beamforming in the array near field from a set of wirelessly syntonized nodes. Previously, we demonstrated near-field beamforming using physically wired syntonization [11], and while prior works have demonstrated far-field or endfire beamforming using open-loop systems [8], [9], this work is, to the best of our knowledge, the first to demonstrate focusing multiple beams or beams and nulls in the near field of an open-loop, wirelessly synchronized distributed array. We demonstrate multiobjective beamforming from a four-antenna array implemented in software-defined radios (SDRs) at 0.9 GHz to two receivers at various positions in the near field. We wirelessly syntonize the nodes using a simple one-way frequency transfer technique with the same antennas that are used for beamforming. This work represents a critical component of distributed beamforming systems that, when combined with relative positioning technologies, will provide a framework for future feedback-free distributed antenna arrays.

II. NEAR-FIELD MULTIOBJECTIVE BEAMFORMING

Multiobjective beamforming has been studied extensively for far-field applications in the literature [12], [13]. The

2771-957X © 2023 IEEE. Personal use is permitted, but republication/redistribution requires IEEE permission. See https://www.ieee.org/publications/rights/index.html for more information.

linear constraint minimum variance (LCMV) [14], [15] and linear constraint minimum power (LCMP) [16] processes have been shown to reduce distortion in the main beam while successfully placing nulls at any desired direction. The LCMV process along with the minimum variance distortionless response (MVDR) has been used in acoustics for speech enhancement [17], and as noise reduction filters [18]. Another application for this process can be found in medical field where LCMV has been used for microwave imaging for clear detection of cancerous tissues [19]. The open-loop topology that we are considering requires multiobjective beamforming processes, which can steer beams and nulls arbitrarily at any given location, making sure that the mainbeam is distortionless. The quiescent pattern constraint is a specialized version of the LCMP process, which provides the optimum beampattern when white noise is present in the system [16]. Since this process is based only on relative phasing of the signals, it is a good candidate for near-field distributed arrays beamforming. In this letter, we use the quiescent LCMP for near-field multiobjective beamforming to steer two beams and then to steer a beam and a null, with a moving receiver node, to demonstrate experimentally both near-field multiobjective beamforming and wireless frequency syntonization of two transmitter nodes using the same antennas for beamforming and for frequency syntonization.

The classical method of quiescent pattern LCMP [16] uses the null constraint matrix C to evaluate the weights required for multiobjective beamforming. C is an $N \times M$ matrix, where N is the number of transmitters, and M is the number of targets at which it is desired to steer beams or nulls; thus, the columns in C are linearly independent of each other. The beamforming and null forming weights are given by $\mathbf{w}_{\text{lcmp}} = \mathbf{g}^H (\mathbf{C}^H \mathbf{C})^{-1} \mathbf{C}^H$, where (.)^H represents the Hermitian operation. For N number of transmitters, the constraint matrix is modeled by the vector containing channel weights of each target M, where M = 1, 2, ..., N - 1, and is given by $\mathbf{C}_{N\times M} = [\mathbf{v}_{1,N} \mid \ldots \mid \mathbf{v}_{m,N} \mid \ldots \mid \mathbf{v}_{M,N}]$. The weights of the channels are given by $\mathbf{v}_{m,n} = e^{-jkr_{mn}}$, where r_{nm} is the distance between transmitters and target locations. We use estimates of the relative positions of the elements to calculate $r_{nm} = ((x_{tx_n} - x_{rx_m})^2 + (y_{tx_n} - y_{rx_m})^2)^{1/2}$, where (x_{tx}, y_{tx}) are the estimated locations of transmitters, and (x_{rx}, y_{rx}) are the target locations. While not demonstrated in this work, the transmitter locations can be estimated via high-accuracy range measurements [20], [21], [22]. The vector $\mathbf{g} = [B_1 \mid \dots \mid B_m \mid \dots \mid B_M]^T$ determines beams or nulls, i.e., $B_m = 1$ for beamforming and $B_m = 0$ for null forming at target location m.

III. NEAR-FIELD BEAMFORMING EXPERIMENTS

Beamforming experiments were conducted using three Ettus Research USRP X310 SDRs, each equipped with two transceivers (UBX-160 daughterboards), each of which used a PulseLarsen SPDA24700/2700 dipole antenna. Two SDRs were designated as transmitters with two transmitting antennas on each, four transmitters in total, and one SDR as receiver with two antennas; the setup is shown in Fig. 1.

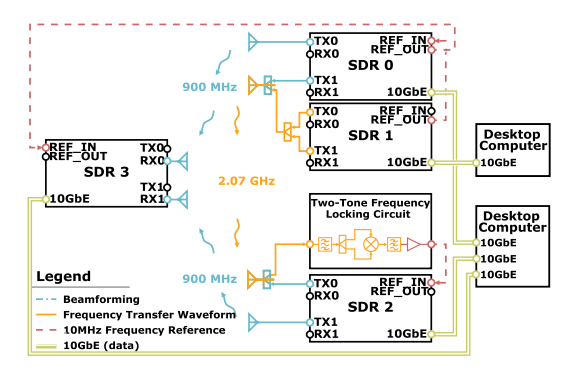


Fig. 1. Schematic of the experimental setup.

Two multiobjective tests were performed: steering two beams (test A) and steering a beam and a null (test B) for moving receivers, while the transmitting nodes were wirelessly syntonized. One antenna on each node was used for the frequency syntonization, with one transmitting the two-tone signal and the other receiving it, while all four antennas were simultaneously performing beamforming. While in [9] the frequency locking was done using directional horn antennas to control the secondary transmitting node, in this letter, we use the same dipole antennas to simultaneously beamform and syntonize the transmitting nodes. Node locations were determined manually; in future work, this will be replaced with microwave wireless localization [20], [21], [22].

A. Wireless Frequency Syntonization

There are multiple ways of frequency locking transmitting nodes for distributed antenna array systems [11]. In this work, we use the beamforming antennas to jointly transfer signals used for syntonization. The concept is based on the transfer of a two-tone signal where the tone separation is equal to the desired frequency reference, which, in this work, is 10 MHz. The secondary node uses a self-mixing circuit [23] to directly demodulate the frequency reference, which can then be input to a phase-locked loop on the secondary node.

Fig. 2 shows the block diagram of the self-mixing circuit consisting of an RF low noise amplifier (LNA) with a gain of 20 dB and a noise figure of 1.5 dB, which boosts the 2.07-GHz signal from -30 to -10 dBm. This was then passed through a cavity filter that filters out spurious signals. The output of the second LNA was fed to the power splitter, which provides inputs to the RF and the LO of the mixer; to prevent the mixer from saturating, the RF was attenuated by a 10-dB attenuator. The output of the mixer was passed through a low-pass filter (LPF) with a cutoff at 11 MHz and then amplified by 40 dB using two 20-dB baseband amplifiers with a noise figure of 2.9 dB each, to make sure that the reference signal was between 0 and 15 dBm, which is needed by USRP X310 SDRs. The output of this mixing circuit had a power level of 10 dBm after 3 dB attenuation, which was then fed into the secondary SDR reference input (REF IN).

B. Experimental Configuration

Experiments were conducted in an indoor environment. The space was an open room; however, no attempt was made to

Fig. 2. Version of the self-mixing circuit schematic given in [23]. A two-tone signal separated by 10 MHz is self-mixed to demodulate a 10-MHz reference signal. The other tones are filtered by the LPF and then amplified to a power between 0 and 15 dBm and fed to the REF IN of the secondary SDR.

TABLE I
RECEIVER POSITIONS DURING BEAMFORMING EXPERIMENTS

Position #	RX0 (x,y) (m)	RX1 (x,y) (m)
1	(-0.20,0)	(-0.07,0)
2	(-0.10,0)	(0.03,0)
3	(0,0)	(0.13,0)
4	(0.10,0)	(0.23,0)
5	(0.20,0)	(0.33,0)

reduce the impact of environmental signals using microwave absorbers. The experiment was designed as shown in Fig. 3. The two-tone signal with a center frequency of 2.07 and 2.08 GHz was generated by SDR 0, controlled by LabView through a 10-Gb Ethernet connection to the desktop computer, and was transmitted by TX2; the signal was received by TX3 and passed through the frequency-locking circuit to input the 10 MHz at REF IN of the SDR 2. The cavity bandpass filter used in the frequency locking circuit operates in the range of 2.03–2.115 GHz. The beamforming transmitter SDRs and the receiving node SDR were controlled using LabView from a separate desktop computer. The beamforming experiment was conducted at a carrier of 900 MHz with a 100-kHz continuous-wave (CW) sideband frequency, so that the baseband signal could be easily sampled and processed at the receiving node.

The two multiobjective tests were Test A: beamform at both RX0 and RX1; and Test B: beamform at RX0 and null form at RX1. The transmit antennas were implemented on two separate tripods to support wide electrical separations of the elements. Each antenna transmitted at a power level of −15 dBm. The transmit antenna pairs TX1/TX2 and TX3/TX4 were each separated by 0.65 m, while the TX2 and TX3 were separated by 0.675 m. The receive antennas RX0 and RX1 were separated by 0.127 m, as they were placed directly on the SDR ports. The receiver node and the centroid of the transmitter nodes were separated by an average distance of 1.91 m. The entire distributed antenna array length was set to 1.95 m with the far-field distance being 22.18 m, making the receiver distance in the near field to the array. However, since the far-field of each individual transmitter element was 0.64 m, the receivers were in the far-field of the individual nodes; thus, only the phase errors due to array propagation needed correction. The receiver antennas were moved to five different positions (Table I) to evaluate the effectiveness of the multiobjective algorithms with different propagation channels.

C. Experimental Results

The results of the two experimental tests are in Fig. 4, where the ratio of the received power when the LCMP algorithm is applied to the maximum power received by RX0 (-16.03 dBm) is shown as a function of receiver position

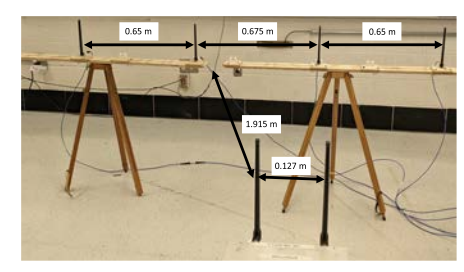


Fig. 3. Experimental setup for the simultaneous frequency syntonization and near-field multiobjective beamforming with distances between transmit and receive elements.

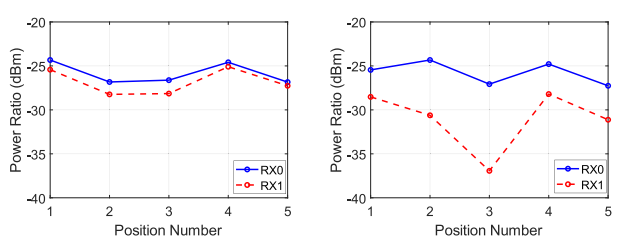


Fig. 4. Experimental results showing the received power at RX0 and RX1 for (left) Test A: beamforming at RX0 and RX1, and (right) Test B: beamforming at RX0 and null forming at RX1.

(refer to Table I for antenna locations). Fig. 4 (left) shows the results of Test A, where the distributed array steered two beams to the receiving locations. The received signal power RX0 and RX1 node averaged -25.84 and -26.83 dBm, respectively, and varied by less than 3 dBm. The variation in received power was due to multipath interference in the uncontrolled laboratory environment. Fig. 4 (right) shows the results of Test B, where a beam and a null were steered to the receivers. In this experiment, RX0 (which received the beam) had an average power of -25.78 dBm and varied by 0.06 dBm, while RX1 (which received the null) had an average power of -31.07 dBm and varied by 5.29 dBm. Variations versus positions were again due to multipath. Despite this, it is clear that the wirelessly syntonized system supports multiobjective beamsteering, demonstrating the feasibility of open-loop distributed beamforming in the near field.

IV. CONCLUSION

We demonstrated open-loop multiobjective microwave beamforming and null forming in the array near field using a wirelessly syntonized distributed antenna array. The results demonstrate the ability to maintain multiple beams or beams and nulls in the near field of a distributed antenna array in a typical indoor environment even when the receiver is moving. Multipath interference was noticeable in the measurements but was not significantly detrimental; in highly cluttered environments, multipath interference may be more significant. These results demonstrate the feasibility of an important component of open-loop distributed beamforming systems that, when combined with other coordination technologies for phase and time synchronization, provides a framework for open-loop distributed beamforming at any distance from the array.

REFERENCES

[1] E. Jovanov, A. O. Lords, D. Raskovic, P. G. Cox, R. Adhami, and F. Andrasik, "Stress monitoring using a distributed wireless intelligent sensor system," *IEEE Eng. Med. Biol. Mag.*, vol. 22, no. 3, pp. 49–55, May/Jun. 2003.

- [2] Y. Kim, R. G. Evans, and W. M. Iversen, "Remote sensing and control of an irrigation system using a distributed wireless sensor network," *IEEE Trans. Instrum. Meas.*, vol. 57, no. 7, pp. 1379–1387, Jul. 2008.
- [3] Z. Iqbal, K. Kim, and H.-N. Lee, "A cooperative wireless sensor network for indoor industrial monitoring," *IEEE Trans. Ind. Informat.*, vol. 13, no. 2, pp. 482–491, Apr. 2017.
- [4] H. Ochiai, P. Mitran, H. V. Poor, and V. Tarokh, "Collaborative beamforming for distributed wireless ad hoc sensor networks," *IEEE Trans. Signal Process.*, vol. 53, no. 11, pp. 4110–4124, Nov. 2005.
- [5] R. Mudumbai, B. Wild, U. Madhow, and K. Ramchandran, "Distributed beamforming using 1 bit feedback: From concept to realization," in *Proc.* 44th Allerton Conf. Commun., Control Comput., vol. 8. Princeton, NJ, USA: Citeseer, 2006, pp. 1020–1027.
- [6] D. R. Brown III and H. V. Poor, "Time-slotted round-trip carrier synchronization for distributed beamforming," *IEEE Trans. Signal Process.*, vol. 56, no. 11, pp. 5630–5643, Nov. 2008.
- [7] S. R. Mghabghab, S. M. Ellison, and J. A. Nanzer, "Open-loop distributed beamforming using wireless phase and frequency synchronization," *IEEE Microw. Wireless Compon. Lett.*, vol. 32, no. 3, pp. 234–237, Mar. 2022.
- [8] S. M. Ellison, S. R. Mghabghab, and J. A. Nanzer, "Multinode open-loop distributed beamforming based on scalable, highaccuracy ranging," *IEEE Sensors J.*, vol. 22, no. 2, pp. 1629–1637, Jan. 2022.
- [9] S. R. Mghabghab and J. A. Nanzer, "Open-loop distributed beamforming using wireless frequency synchronization," *IEEE Trans. Microw. Theory Techn.*, vol. 69, no. 1, pp. 896–905, Jan. 2021.
- [10] J. M. Merlo and J. A. Nanzer, "High accuracy wireless time synchronization for distributed antenna arrays," in *Proc. IEEE Int. Symp. Anten*nas Propag. USNC-URSI Radio Sci. Meeting (AP-S/URSI), Jul. 2022, pp. 1966–1967.
- [11] A. Bhattacharyya, S. R. Mghabghab, S. Vakalis, and J. A. Nanzer, "Experimental implementation of microwave multi-objective linear constrained minimum power beamforming in the near field," in *Proc. IEEE Int. Symp. Antennas Propag. USNC-URSI Radio Sci. Meeting (AP-S/URSI)*, Jul. 2022, pp. 1974–1975.

- [12] S. Pulipati, V. Ariyarathna, M. R. Khan, S. Bhardwaj, and A. Madanayake, "Aperture-array & lens+FPA multi-beam digital receivers at 28 GHz on Xilinx ZCU 1275 RF SoC," in *IEEE MTT-S Int. Microw. Symp. Dig.*, Aug. 2020, pp. 555–558.
- [13] V. Ariyarathna et al., "Multi-beam 4 GHz microwave apertures using current-mode DFT approximation on 65 nm CMOS," in *IEEE MTT-S Int. Microw. Symp. Dig.*, May 2015, pp. 1–4.
- [14] J. Capon, "High-resolution frequency-wavenumber spectrum analysis," Proc. IEEE, vol. 57, no. 8, pp. 1408–1418, Aug. 1969.
- [15] O. L. Frost, "An algorithm for linearly constrained adaptive array processing," *Proc. IEEE*, vol. 60, no. 8, pp. 926–935, Aug. 1972.
- [16] H. V. Trees, Optimum Array Processing. Hoboken, NJ, USA: Wiley, 2002.
- [17] E. A. P. Habets, J. Benesty, S. Gannot, P. A. Naylor, and I. Cohen, "On the application of the LCMV beamformer to speech enhancement," in *Proc. IEEE Workshop Appl. Signal Process. Audio Acoust.*, Oct. 2009, pp. 141–144.
- [18] M. Souden, J. Benesty, and S. Affes, "A study of the LCMV and MVDR noise reduction filters," *IEEE Trans. Signal Process.*, vol. 58, no. 9, pp. 4925–4935, Sep. 2010.
- [19] W. Zhi, F. Chin, and M. Chia, "Near field UWB LCMV imaging for breast cancer detection with entropy based artifacts removal," in *Proc.* IEEE Int. Conf. Acoust. Speech Signal Process., vol. 2, May 2006, p. 2.
- [20] A. Schlegel, S. M. Ellison, and J. A. Nanzer, "A microwave sensor with submillimeter range accuracy using spectrally sparse signals," *IEEE Microw. Wireless Compon. Lett.*, vol. 30, no. 1, pp. 120–123, Jan. 2020.
- [21] S. R. Mghabghab and J. A. Nanzer, "Localization in distributed wireless systems based on high-accuracy microwave ranging," in *Proc. IEEE-APS Top. Conf. Antennas Propag. Wireless Commun. (APWC)*, Aug. 2021, pp. 122–125.
- [22] S. R. Mghabghab and J. A. Nanzer, "Impact of localization error on open-loop distributed beamforming arrays," in *Proc. XXXIV Gen. Assem.* Sci. Symp. Int. Union Radio Sci. (URSI GASS), Aug. 2021, pp. 1–3.
- [23] S. Mghabghab and J. A. Nanzer, "A self-mixing receiver for wireless frequency synchronization in coherent distributed arrays," in *IEEE MTT-S Int. Microw. Symp. Dig.*, Aug. 2020, pp. 1137–1140.